An Accurate Measurement of the Landau-Pomeranchuk-Migdal Effect

P. L. Anthony,[1] R. Becker-Szendy,[1] P. E. Bosted,[2] M. Cavalli-Sforza,[3,*] L. P. Keller,[1] L. A. Kelley,[3] S. R. Klein,[3,4] G. Niemi,[1] M. L. Perl,[1] L. S. Rochester,[1] and J. L. White[1,2]

[1]*Stanford Linear Accelerator Center, Stanford, California 94309*

[2]*The American University, Washington, D.C. 20016*

[3]*Santa Cruz Institute for Particle Physics, University of California, Santa Cruz, California 95064*

[4]*Lawrence Berkeley Laboratory, Berkeley, California 94720*

(Received 1 May 1995)

In the 1950s, Landau, Pomeranchuk, and Migdal (LPM) predicted that the cross section for bremsstrahlung from highly relativistic particles in dense media would be suppressed due to interference between amplitudes of nearby interactions. We have measured the production rates of 5 to 500 MeV photons from 8 and 25 GeV electrons traversing thin gold and carbon targets. We observe, to within 5% accuracy, suppression at the level predicted by Migdal. For extremely thin targets, we observe "edge effects" where the LPM suppression is reduced near the edges of the targets. We also point out the imprecise foundation of the LPM theory.

PACS numbers: 41.60.–m, 12.20.Fv

In the 1950s Landau, Pomeranchuk, and Migdal (LPM) [1,2] predicted that the cross section for bremsstrahlung from highly relativistic particles in dense media is suppressed due to interference between amplitudes of nearby interactions. The suppression has its roots in the uncertainty principle. The kinematics of bremsstrahlung requires that the longitudinal momentum transfer between the nucleus and the electron must be small; the uncertainty principle then requires that the interaction must occur over a large longitudinal distance scale (formation zone). If the electron Coulomb scatters while traversing this zone, the bremsstrahlung amplitude from before and after the scattering can interfere, reducing the amplitude for bremsstrahlung photon emission.

We present here the first quantitative measurement of bremsstrahlung suppression due to the LPM effect. In the past there have been several qualitative tests of the LPM effect using cosmic rays and one qualitative test at an accelerator [3]. The effect is relevant in many areas, but particularly in high energy cosmic ray air showers [4]. Our experiment, SLAC E-146 [5,6], carried out at the Stanford Linear Accelerator Center (SLAC), studied the bremsstrahlung production of 5 to 500 MeV photons by 8 and 25 GeV electrons. We found that the suppression of bremsstrahlung predicted by the LPM theory is correct to within 5%.

Unfortunately, no concise derivations of the LPM effect exist. Qualitative discussions have been given by Galitsky and Gurevich [7] and by Perl [8]. Here we give a brief qualitative discussion and the basic equations. The differential cross section for the bremsstrahlung production of a photon of energy k by an ultrarelativistic electron of energy E and mass m, where $k \ll E$ (complete screening) [9] is given by

$$\frac{d\sigma_{\mathrm{BH}}}{dk} = \frac{4\alpha r_e^2}{3k}\left[\{y^2 + 2[1 + (1 - y)^2]\} \times (Z^2 F_{\mathrm{el}} + Z F_{\mathrm{inel}}) + (1 - y)\frac{(Z^2 + Z)}{3}\right]. \quad (1)$$

Here $y = k/E$, α is the fine structure constant, r_e is the classical radius of the electron, and Z is the nuclear charge. $F_{\mathrm{el}} \approx \ln(184/Z^{1/3})$ and $F_{\mathrm{inel}} \approx \ln(1194/Z^{2/3})$ are the elastic and inelastic atomic from factors [9]. Equation (1) has the well-known Bethe-Heitler form $(d\sigma_{\mathrm{BH}}/dk)_{y \ll 1} \sim 1/k$.

In this kinematic regime $k \ll E$ the average angle between the incident electron and the produced photon is small, $\theta_k \approx mc^2/E$, and the average angle between the scattered electron and the incident electron is smaller still. Neglecting these angles, the longitudinal momentum transfer to the atom is $q_{\parallel} \approx k/2\gamma^2 c$, where $\gamma = E/mc^2$ [8]. The uncertainty principle then requires that the spatial position of the bremsstrahlung process has a longitudinal uncertainty of $L_{\parallel} = \hbar/q_{\parallel} \approx 2\hbar c\gamma^2/k$. In alternate language, the electron and photon slowly split apart over the distance $L_{\parallel}$. In a sufficiently dense medium the electron mean free path is much less than $L_{\parallel}$, so an electron will interact while traversing $L_{\parallel}$; in the LPM effect the relevant interaction is multiple scattering. Roughly, bremsstrahlung is suppressed [7] when the mean square multiple scattering angle over the distance $L_{\parallel}$

$$\theta_s^2 = \left(\frac{E_s}{E}\right)^2 \frac{L_{\parallel}}{X_0} \quad (2)$$

is greater than or equal to θ_k^2. Here $E_s = mc^2(4\pi/\alpha)^{1/2} \approx 21$ MeV and X_0 is the radiation length. Therefore $d\sigma/dk$ is suppressed when

$$k < k_{\mathrm{LPM}} = \frac{E^2}{E_{\mathrm{LPM}}}, \quad (3)$$

0031-9007/95/75(10)/1949(4)$06.00

where $E_{\mathrm{LPM}} = mc^4 X_0 \alpha / 8\pi\hbar c = (3.8 \times 10^{12}\ \mathrm{eV}) X_0$ (cm).

Table I shows that as Z increases E_{LPM} decreases and k_{LPM}, the electron energy dependent upper limit for the LPM effect, increases. Using semiclassical arguments [1], it can be shown that, for $y \ll 1$, $d\sigma_{\mathrm{LPM}}/dk \sim 1/\sqrt{k}$ in contrast to $d\sigma_{\mathrm{BH}}/dk$, which is proportional to $1/k$. A more accurate analysis becomes very involved; Migdal based his calculations on scattering theory.

In his formulation [2], Migdal defines a dimensionless variable

$$s = \frac{1}{2}\left(\frac{y}{1-y}\right)^{1/2}\left(\frac{mc}{\hbar}\,\frac{mc^2}{E}\,\frac{\alpha X_0}{8\pi\xi(s)}\right)^{1/2}, \qquad (4)$$

where $1 \le \xi(s) \le 2$. When $y \ll 1$, $s \sim (L_{\mathrm{LPM}}/L_{\|})^{1/2}$. When $s \gg 1$, $d\sigma/dk$ is unaffected; when $s \ll 1$, there is strong suppression. Migdal found that

$$\frac{d\sigma_{\mathrm{LPM}}}{dk} = \frac{4\alpha r_e^2 \xi(s)}{3k}\{y^2 G(s) + 2[1 + (1-y)^2] \times \phi(s)\} Z^2 \ln\left(\frac{184}{Z^{1/3}}\right), \qquad (5)$$

where $G(s)$ and $\phi(s)$ may be approximated by sums [4]. In the no suppression limit $s \to \infty$, $G(s) \to 1$, and $\phi(s) \to 1$. Comparing $d\sigma_{\mathrm{LPM}}/dk$ [Eq. (6)] with $d\sigma_{\mathrm{BH}}/dk$ [Eq. (1)] in this limit, $d\sigma_{\mathrm{LPM}}/dk$ yields the $Z^2 F_{\mathrm{el}}$ term but not the ZF_{inel} or the $Z^2 + Z$ terms. Our calculations include the ZF_{inel} term by normalizing both our $d\sigma_{\mathrm{LPM}}/dk$ and $d\sigma_{\mathrm{BH}}/dk$ to the radiation length as defined by Tsai [9]. The $Z^2 + Z$ term is omitted from both our cross sections and the definition of the radiation length [9]; this is roughly a 2% correction.

Figure 1 shows the suppression of the LPM cross section as k decreases. Right above the region where the suppression disappears, $d\sigma_{\mathrm{LPM}}/dk$ rises slightly above $d\sigma_{\mathrm{BH}}/dk$; this occurs because $\xi(s)\phi(s)$ rises slightly above 1.

The experimental layout is shown in Fig. 2. Electron beams with energies of 8 or 25 GeV entered the SLAC end station A and interacted in targets of thicknesses 0.1%–6% X_0. The electrons were then magnetically bent downward by 39 mrad (at the full beam energy) into a wire chamber spectrometer and then into lead glass blocks which accurately count the electrons. Photons produced in the target were detected 50 m downstream in a BGO calorimeter array. To minimize backgrounds, the electron path upstream of the calorimeter and the photon flight path were kept in vacuum. The beam ran at 120 pulses/sec,

TABLE I. Z, X_0, L_{LPM}, and k_{LPM}, the latter for 25 GeV electrons.

Target	Z	X_0 (cm)	E_{LPM} (TeV)	k_{LPM} (MeV)
C	6	18.8	71	8.8
Au	79	0.33	1.25	500

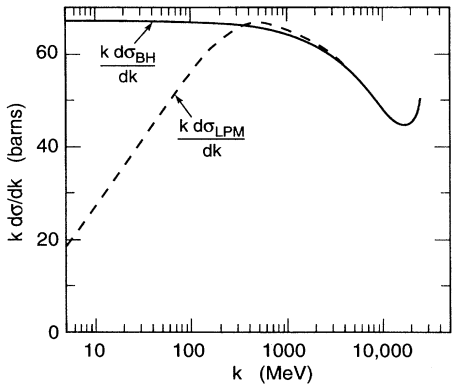

FIG. 1. Comparison of $kd\sigma_{\mathrm{LPM}}/dk$ and $kd\sigma_{\mathrm{BH}}/dk$ for 25 GeV electrons incident on a uranium target. The cross sections are not corrected for the edge effect.

with an intensity adjusted to average 1 electron/pulse, except for the 0.1% gold target, where higher rates were sometimes used. The beam was generated parasitically during SLC collider operation [10]. To avoid possible trigger bias, data were recorded at every pulse. This Letter discusses data taken with gold and carbon targets, as detailed in Table II.

The BGO calorimeter comprises 45 crystals (a 7 by 7 array, with the corners missing). Each crystal is 2 cm square by 20 cm ($18X_0$) deep. The calorimeter was read out by photomultiplier tubes (PMTs), which detected about one photoelectron per 30 keV of energy deposition. The PMT signals were digitized by LeCroy 2282, 12 bit ADCs, with the phototube gain adjusted so that one count was about 100 keV. The FWHM calorimeter resolution was 6% for 400 MeV electrons, rising to 8% FWHM for 40 MeV electrons. Three methods were used for calorimeter calibration: electron beams with energies of 400 and 500 MeV; cosmic ray muons; and event reconstruction, requiring that the photon energy in the BGO and the electron energy measured in the wire chamber sum to the beam energy. The BGO temperature was monitored during data taking, and the BGO data were

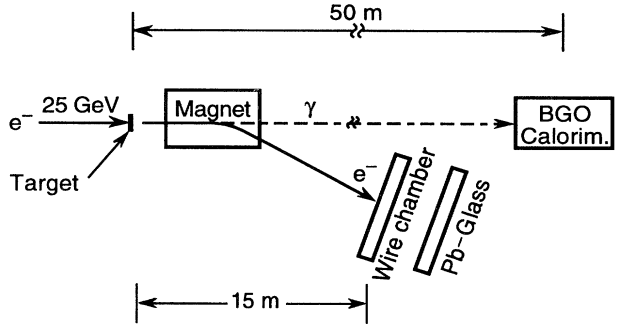

FIG. 2. Schematic picture of the experiment.

TABLE II. Target thickness t in mm, g/cm^2, and X_0.

Target	6% C	0.1% Au	0.7% Au	6% Au
t (mm)	11.732	0.0039	0.0231	0.1991
t (g/cm^2)	2.5717	0.0074	0.0445	0.384
t (X_0)	0.0602	0.0011	0.0068	0.0591

corrected to compensate for temperature variations, using the measured temperature response. Further details of the calibration are provided in Refs. [5] and [6].

Our analysis selected bremsstrahlung events containing a photon in the calorimeter plus a single electron in the lead glass blocks. The photon energies were then histogrammed. Figure 3 shows a sampling of our data,

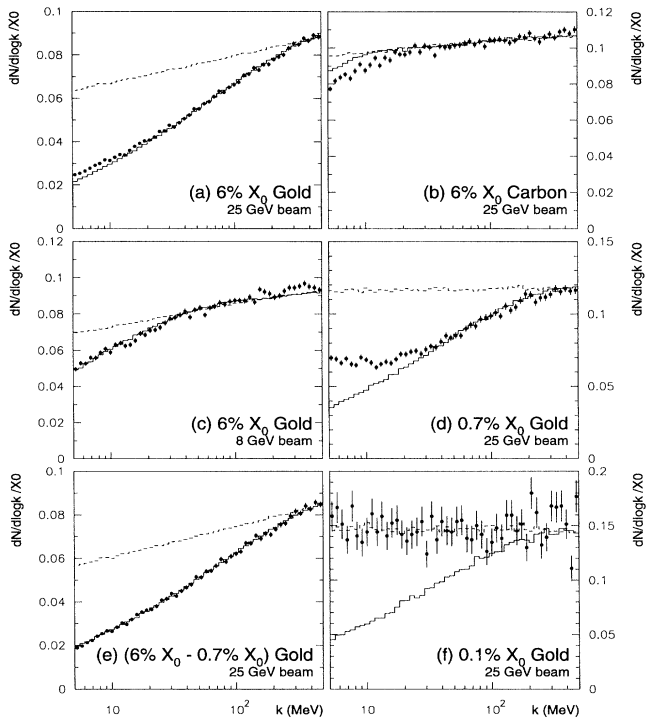

FIG. 3. Measurements with statistical errors only of $dN/d(\log k)$ compared with Monte Carlo calculated theoretical curves. The cross sections are given in terms of $dN/[d(\log k)/X_0]$, where N is the number of events per photon energy bin per incident electron. The photon energy scale is logarithmic with 25 bins per decade, so each bin has a width $\Delta k \sim 0.0964k$. The dashed histogram is the Bethe-Heitler Monte Carlo prediction, and the solid line gives the LPM Monte Carlo prediction. (a) 25 GeV electrons incident on 6% X_0 gold; (b) 25 GeV electrons incident on 6% X_0 carbon; (c) 8 GeV electrons incident on 6% X_0 gold; (d) 25 GeV electrons incident on 0.7% X_0 gold; (e) data and Monte Carlo curves from 25 GeV electrons incident on 0.7% X_0 gold subtracted from 25 GeV electrons incident on 6% X_0 gold, leaving the "middle" 5.3% X_0 of gold; (f) 25 GeV electrons incident on 0.1% X_0 gold.

together with Monte Carlo predictions, for both the Bethe-Heitler and LPM $dN/d(\log k)$. The plots show $dN/d(\log k)$, with 25 bins per decade of energy, so that the bin width $\Delta E \approx 0.09E$. Logarithmic bins are used so that the Bethe-Heitler $1/k$ cross section appears roughly flat.

Figures 3(a) and 3(b) show the number of observed photons per 25 GeV electron traversing the 6% X_0 gold and carbon targets. The gold target shows a large suppression compared to the Bethe-Heitler prediction (dashed lines). Carbon, which is much less dense, shows little suppression. Figure 3(c) shows the corresponding plots for 8 GeV electrons incident on the gold target; here the LPM effect is much reduced. In all three cases, excellent agreement is seen with the Monte Carlo LPM curves (solid lines) above $k = 30$ MeV; below 30 MeV the data are higher than the LPM Monte Carlo.

One shortcoming in Migdal's formulas is that they apply only for infinitely thick targets. In a target of finite thickness, electrons may interact near an edge. Then the formation zone may extend out of the target so the electrons undergo less multiple scattering, and therefore less suppression. Unfortunately, we have found no satisfactory theoretical treatment of this phenomenon. This can explain the discrepancy between the LPM prediction and data below about 30 MeV in Fig. 3(a). This effect is proportionately much larger in thinner targets, as seen in Fig. 3(d) for 25 GeV electrons incident on a 0.7% X_0 gold target. To remove edge effects from our data, we subtract the 0.7% X_0 gold target data from the 6% X_0 gold data to get the middle 5.3%, without edge effects. The result is shown in Fig. 3(e). Repeating this procedure with Monte Carlo results accounts for multiple photon emission; the agreement is excellent over the entire range $5 < k < 500$ MeV. This procedure introduces a small (<2%) systematic error due to additional multiphoton emission associated with the edge effect.

For extremely thin targets, thinner than the formation zone length, LPM suppression should completely disappear because there is too little total multiple scattering to cause suppression. This effect is verified by the data shown in Fig. 3(f) from 25 GeV electrons passing through a 0.1% X_0 target.

The errors shown on the plots are statistical only. The point-to-point systematic errors vary slowly with k and correspond to a 4.5% uncertainty across the measured range of k. The major sources are photon cluster finding (2%), calorimeter energy calibration (1.5%), calorimeter nonlinearity (3%), backgrounds (1%), uncertainty in the target density (2%), and multiphoton pileup due to the edge effect (1%).

The major backgrounds—synchrotron radiation from the spectrometer and beam line magnets, and transition radiation in the target—are expected to be small above 5 MeV. The synchrotron radiation and other beam related backgrounds have been measured in empty target holder

runs and found to be small, below 0.1% per electron. When significant (as for the 0.1% gold target), they have been subtracted from the corresponding target-in data.

The major difference between the Monte Carlo curves and the theoretical cross sections (Fig. 1) is that the Monte Carlo includes the effect of multiphoton emission, where a single electron passing through the target interacts twice, emitting two different photons. This depresses the low energy end of the spectrum and increases the high energy end, tilting the otherwise fairly flat Bethe-Heitler spectrum. The Monte Carlo includes possible photon absorption in the target and smearing to simulate calorimeter resolution. At low energies, we include an additional suppression due to the longitudinal density effect [11], following the prescription in Ref. [2].

The Monte Carlo curves are normalized so that the LPM curves match the data in the region $450 < k < 500$ MeV. Except for the 0.1% X_0 gold, the data are consistent with a common normalization factor of $0.94 \pm 0.01 \pm 0.032$. The 3.2% systematic error comes from uncertainties in the target thickness (2%), energy calibration (1%), electron flux (0.5%), Monte Carlo (excluding bremsstrahlung physics input) (1%), and normalization technique (2%).

It is difficult to explain a 6% normalization difference in terms of experimental biases alone. The difference is likely due to the approximate nature of these formulas. Radiative corrections could be significant at this level because E/k is so large. Because the longitudinal density effect suppresses low energy photons, the exact corrections are unknown. There are also shifts from neglecting the $Z(Z + 1)/3$ term in the Tsai formula, and because the electron distribution in solids differs from the free atom wave functions used in screening calculations.

In summary, we have found that the Migdal theory of the LPM effect accurately describes data taken on carbon and gold targets, once multiphoton pileup and edge effects are taken into account. The suppression varies with both target X_0 and electron energy as predicted by Migdal. For thin targets, edge effects reduce the suppression. For all of our data, the absolute bremsstrahlung rate is slightly below that predicted by current theory. More theoretical work is called for to accurately treat these edge effects, and the small but significant normalization difference between data and theory needs to be better understood.

We would like to thank the SLAC Experimental Facilities group for their assistance in setting up the experiment and the SLAC Accelerator Operators group for their efficient beam delivery. Walter Meyerhof provided the target holder. This work was supported by Department of Energy Contracts DE-AC03-76SF00515 (SLAC), DE-AC03-76SF00098 (LBL), W-4705-ENG-48 (LLNL), and National Science Foundation Grants NSF-PHY-9113428 (UCSC) and NSF-PHY-9114958 (American U.).

*Present address: Institut de Fisica d'Altes Energies, Universitat Autonima de Barcelona, 08193 Bellaterra (Barcelona), Spain.

[1] L. D. Landau and I. J. Pomeranchuk, Dokl. Akad. Nauk. SSSR **92**, 535 (1953); **92**, 735 (1953). These two papers are available in English in L. Landau *The Collected Papers of L. D. Landau* (Pergamon Press, New York, 1965).

[2] A. B. Migdal, Phys. Rev. **103**, 1811 (1956).

[3] A. Varfolomeev *et al.,* Sov. Phys. JETP **42**, 218 (1976).

[4] T. Stanev *et al.,* Phys. Rev. D **25**, 1291 (1982).

[5] S. R. Klein *et al.,* in *Lepton and Photon Interactions,* edited by P. Drell and D. Rubin, AIP Conf. Proc. No. 302 (AIP, New York, 1994), p. 172.

[6] R. Becker-Szendy *et al.*, in Proceedings of the 21st SLAC Summer Institute on Particle Physics, Palo Alto, 1994 (to be published), p. 519.

[7] V. M. Galitsky and I. I. Gurevich, Il Nuovo Cimento **32**, 396 (1964).

[8] M. L. Perl, in *Proceedings of the 1994 Les Rencontres de Physique de la Vallee D'Aoste,* edited by M. Grego (Editions Frontieres, Gif-sur-Yvette, France, 1994), p. 567.

[9] Y.-S. Tsai, Rev. Mod. Phys. **46**, 815 (1974).

[10] M. Cavalli-Sforza *et al.,* IEEE Trans. Nucl. Sci. **41**, 1374 (1994).

[11] M. L. Ter-Mikaelian, Dokl. Akad. Nauk. SSR **94**, 1033 (1954). For a discussion in English, see M. L. Ter-Mikaelian, *High Energy Electromagnetic Processes in Condensed Media* (John Wiley & Sons, New York, 1972).